



BIOMEDICAL SCIENCES

Epigallocatechin gallate-capped gold nanoparticles enhanced the tumor suppressors let-7a and miR-34a in hepatocellular carcinoma cells

SHADY M. MOSTAFA, AMIRA M. GAMAL-ELDEEN, NABILA ABD EL MAKSOUH & ABDELGAWAD A. FAHMI

Abstract: Epigallocatechin gallate (EGCG), major constituent of green tea, possesses antioxidant, antiviral, and anticancer activities. Gold nanoparticles (AuNPs) play an important role in drug delivery due to their stability, ease of surface functionalization, and unique optical properties. This study aimed to investigate the influence of EGCG-capped AuNPs on tumor suppressor miRNAs (miR-34a and let-7a) and their targeted cell death mediators in HepG2 cells, compared with celastrol. EGCG-AuNPs were prepared and characterized. antioxidant activity was estimated by DPPH scavenging assay; cytotoxicity was assessed by MTT assay; let-7a and miR-34a expression was analyzed by qPCR; and miRNAs targets (c-Myc and caspase-3) were assessed by ELISA and immunocytofluorescence, respectively. The average size of EGCG-AuNPs was 35 nm, with a λ_{\max} of ~535 nm. EGCG-AuNPs exerted cytotoxicity on HepG2 cells stronger than that of EGCG alone. EGCG-AuNPs and EGCG presented half-maximal radical scavenging concentrations (SC_{50}) of 539 $\mu\text{g}/\text{ml}$ and 45 $\mu\text{g}/\text{ml}$, respectively. The expression levels of let-7a and miR-34a were significantly elevated in HepG2 cells after EGCG-AuNP treatment for 72 h. c-Myc protein expression was reduced, whereas caspase-3 expression was increased following treatment with EGCG-AuNPs. In conclusion, Au-NPs are effective carrier for EGCG, and EGCG-AuNPs are promising anti-cancer agent.

Key words: EGCG-AuNPs, Hep-G2, miR-34a, let-7a, c-Myc, Caspase-3.

INTRODUCTION

Hepatocellular carcinoma (HCC) comprises approximately 75% of all liver cancer diseases. Current treatments for HCC include surgical resection, transplantation, and chemical therapy (e.g., Sorafenib), which is associated with low disease stabilization, due to acquired resistance (Petrick & McGlynn 2019). Therefore, increasing research has focused on the identification of more effective treatments, including natural product-derived pure compounds. Different types of tea are produced from the leaves of

the *Camellia sinensis* plant (green tea), which have high polyphenolic contents (Zaveri 2006). Catechins are the major constituents in green tea, with epigallocatechin gallate (EGCG) accounting for 65% of total catechins. EGCG has gained attention due to its antioxidant (Hu et al. 2006), antiviral, and antimicrobial (Al-Shaeli et al. 2019) activities, and as an anti-tumor agent that can target tumor cells rather than normal cells (Al-Shaeli et al. 2019, Zan et al. 2019, Tauber et al. 2020, Chen et al. 2019). The structure-function relationship of EGCG, as an anti-cancer agent, has been documented by several studies. The B-ring

(catechol group) possesses potent antioxidant activity (Fig. 1a), and the D-ring (gallate group) is more effective for inducing cytotoxicity and the inhibition of fatty acid synthase in tumor cells, leading to cytotoxic effects (Shammas et al. 2006, Li et al. 2011).

EGCG has poor stability and low bioavailability (Lambert & Yang 2003), particularly under alkaline and neutral conditions, presenting rapid degradation, including the deprotonation of hydroxyl groups and subsequent biotransformation reactions, resulting in the loss of biological activity (Zhu et al. 1997, Sang et al. 2011). The oral bioavailability of EGCG is affected by several factors, such as the high molecular weight, pH, the presence of metal ions, temperature, biometabolic conversions, and oxygen concentration (Mereles & Hunstein 2011).

The high molecular weight of EGCG, the high number of hydroxyl groups, and the presence of a galloyl moiety in EGCG prevent its passage through the intestinal epithelium, resulting in poor bioavailability (Warden et al. 2001). EGCG degradation surges with relative humidity and temperature, further reducing its bioavailability (Li et al. 2011). EGCG is also sensitive to the pH range within the human gastrointestinal tract.

High pH results in EGCG oxidation, which leads to the formation of the dimerized products, known as asinensins, which also reduces EGCG accessibility (Yoshino et al. 1999, Su et al. 2003, Dube et al. 2010). The low bioavailability of EGCG has been associated with other factors, including the highly hydrophilic-lipophobic nature of EGCG metabolism, into methylated, glucuronidated, and sulfate products, and the active elimination of several polyphenolic compounds by multidrug resistance-associated protein 2 (MRP2) (Lu et al. 2003, Hong et al. 2003). Consequently, the development of strategies capable of increasing EGCG bioavailability and stability is highly desirable. Several recent studies have investigated the use of nanomaterials, such as gold nanoparticles (Hsieh et al. 2011), liposomes (Ramadass et al. 2015), albumin (Ramesh & Mandal 2019), folic acid-functionalized nanostructured lipid (Granja et al. 2019), and polymeric nanoparticles (Sanna et al. 2011), for use as EGCG delivery vehicles, to facilitate drug entry, enhance bioavailability, avoid biometabolic modifications, and extend circulation time.

Few clinical trials have been conducted to investigate green tea and the therapeutic effects of EGCG in cancer. A clinical trial explored the

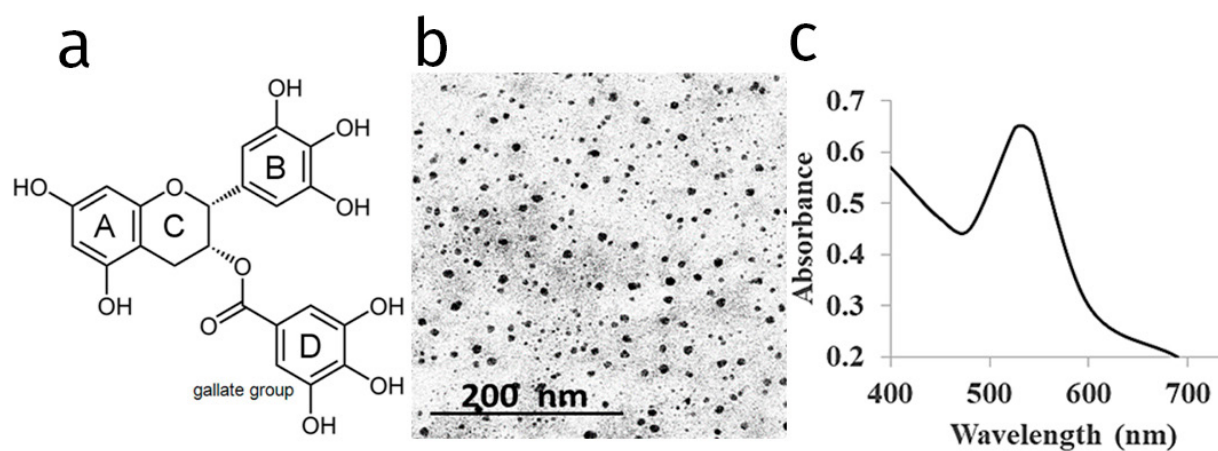


Figure 1. a. The chemical formula of epigallocatechin gallate (EGCG), illustrating the A-, B-, C- and D- rings. **Characterization of EGCG-AuNPs: b.** TEM image of EGCG-AuNPs and **c.** UV-visible spectrum of the prepared EGCG-AuNPs, with a λ_{\max} at 535 nm.

preventive effects of green tea polyphenols against high-risk hepatocellular carcinoma. The results showed that tea polyphenols decreased the levels of urinary 8-hydroxydeoxyguanosine and suppressed DNA damage (Luo et al. 2006). Another phase II clinical trial in China confirmed that the oral administration of EGCG was an effective therapy method for acute radiation-induced esophagitis, which was able to significantly reduce pain in patients and to improve the therapeutic effects (Zhao et al. 2015). A recent phase II, randomized, controlled trial (RCT) was performed to evaluate whether Veregen[®], a topical ointment containing EGCG, was effective for the treatment of usual-type vulvar intraepithelial neoplasia (uVIN), and the results indicated that Veregen[®] application is safe and leads to at least the partial clinical resolution of uVIN lesions (Yap et al. 2019).

Nanomaterials have gained interest for use in drug delivery, due to the simplicity of the mode of action, the ease of surface modification, and other characteristics (Golchin et al. 2018). Gold nanoparticles (AuNPs) present great application potential and capacity for drug delivery, due to prolonged-release kinetics and long-term persistence at multiple, locus-specific target sites utilized in cancer therapy (Golchin et al. 2018). For example, the gold nanoshells, Aurora, have recently received FDA approval for cancer chemotherapy (Guhrenz et al. 2017, Golchin et al. 2018). Additionally, AuNPs have been used in diagnostic probes to detect cancer (Golchin et al. 2018).

AuNPs are widespread nanocarriers in biomedical applications, due to their stability, ease of surface functionalization, and unique optical properties (Verma et al. 2020). AuNPs can be used to target tumor-specific sites through passive accumulation, due to their enhanced permeability and retention (EPR), or through functionalization with an

active-targeting molecule (Chamundeeswari et al. 2019). Recently, EGCG-AuNPs showed a selective inhibitory efficacy in human smooth muscle cells, and the cellular internalization of EGCG-AuNPs within short periods of time was associated with laminin receptor-mediated endocytosis (Khoobchandani et al. 2016, Shukla et al. 2012).

Small single RNA strands, known as micro RNAs (miRNAs), are highly stable, conserved, non-coding transcripts that can post-transcriptionally regulate gene expression (Bach et al. 2017). Studies have demonstrated that miRNAs can functionally regulate many biological processes, including the balance between cell growth and death. The abnormal expression of miRNAs has been associated with numerous human diseases, particularly cancers and many inflammatory conditions (Hata & Lieberman [et al. 2015). miRNAs are expressed at elevated levels in tumors are referred to as oncogenes or oncomiRs, and usually stimulate the development and progression of tumors by reducing the expression of tumor suppressor genes and/or specific genes that regulate cell death/apoptosis and differentiation (Zhang et al. 2007). miRNAs can act as either oncomiRs or tumor suppressors, depending on the context (Zhang et al. 2007). MiR-34a is a tumor-suppressing miRNA that is downregulated in many human cancers, including HCC (Wang et al. 2017, Cai et al. 2017). MiR-34a and let-7a are tumor suppressor miRNAs that are involved in the regulation of many critical genes that participate in the tumorigenesis process, such as caspase-3, c-Myc, and several other genes. Consequently, the induction of miR-34a expression could suppress tumor growth and progression (Bader 2012, Daige et al. 2014).

Celestrol, a well-known chemotherapeutic agent, is a quinone methide triterpenoid, extracted from the roots of *Trypterigium wilfordii*, also

known as the Thunder of God Vine (Kannaiyan et al. 2011). Celestrol inhibits proliferation, induces apoptosis, and suppresses invasion and angiogenesis in various cancer diseases (Pang et al. 2010). The molecular targets of celestrol play various roles in the initiation, proliferation, and progression of carcinogenesis (Kannaiyan et al. 2011). To our knowledge, neither the effects of AuNPs nor EGCG- AuNPs on miRNAs have been previously studied. Therefore, this study aimed to investigate the influence of EGCG-capped AuNPs on tumor suppressor miRNAs (miR-34a and let-7a) and their targeted cell death mediators, compared with the influence of the known anti-cancer drug celestrol.

MATERIALS AND METHODS

Materials

Epigallocatechin gallate (EGCG; 989-51-5, Sigma-Aldrich) was dissolved in phosphate-buffered saline (PBS). Sodium-tetrachloroaurate (NaAuCl₄; 13874-02-7, Sigma-Aldrich) was used to prepare the EGCG-conjugated AuNPs. Celestrol (34157-83-0, Sigma-Aldrich) was used as a positive control, after being dissolved in < 0.1% dimethyl sulfoxide (DMSO), at a safe concentration. All buffers and reagents were analytical-grade (Sigma-Aldrich, USA) unless otherwise mentioned. EGCG-conjugated AuNPs (EGCG-AuNPs) were prepared, as described by Zhu et al. (2019). Transmission electron microscopy (TEM) (Joel Jem-2100), performed with a Malvern Zetasizer Nano ZS instrument, with a He/Ne laser, and absorption spectroscopy (Evolution 300 UV-Vis spectrophotometer, Thermo Scientific, USA) were used to characterize the size and absorption spectrum of EGCG-AuNPs. The *in vitro* stability of the EGCG-AuNPs was tested in phenol red-free Dulbecco's modified Eagle medium (DMEM), both with and without 10% fetal bovine serum (FBS), after 1 h and 24 h. The absorption at 530

nm confirmed the retention of nanoparticles in the medium. The Folin-Ciocalteu colorimetric assay revealed the loading capacity for EGCG on AuNPs (Zhu et al. 2019).

Antioxidant activity

The antioxidant activities of the tested agents (EGCG, EGCG-AuNPs, and celestrol) were investigated by assessing their scavenging capacities against 1,1-diphenyl-2-picryl-hydrazyl (DPPH) radicals, in a non-cellular assay (van Amsterdam et al. 1992). The percentage of DPPH bleaching was used to calculate the half-maximal scavenging concentration (SC₅₀) compared to ascorbic acid.

Cell Viability

Human HCC HepG2 cells (ATCC, Manassas, VA, USA) were propagated in high-glucose DMEM (Biowest, France), after adding 10% FBS (Biowest) and 1% antibiotic/antimycotic cocktail (Biowest, France), and then incubated at 37°C, in humidified air containing 5% CO₂. Monolayer cells, at 70%–80% confluence, were harvested by Trypsin/EDTA (Biowest, France) treatment, at 37°C. The viability of HepG2 cells was assessed using the 3-(4,5-dimethyl-2-thiazolyl)-2,5-diphenyl-2H-tetrazolium bromide (MTT) cell viability assay (Hansen et al. 1989). Cells were incubated with various concentrations of EGCG, EGCG-AuNPs, and celestrol, for different time intervals (24, 48, and 72 h). The relative cell viability was assessed by dissolving the insoluble formazan precipitate (converted from MTT) in DMSO. Absorbance was then measured at 570 nm, using the FLOUstar Optima multi-detection system (BMG, Germany). The data were expressed as the mean percentages of viable cells, relative to non-treated cells, and recorded as the mean ± standard deviation (SD). The half-maximal inhibitory concentration (IC₅₀) was calculated from the dose-dependent curve

for each time point, and afterward, the 72-h time point was selected for further experiments.

Apoptosis-Necrosis assay

HepG2 cells were seeded into 8-well cell culture glass slides (SPL life sciences, Korea), at 5×10^3 cells per well. Cells were treated with EGCG, EGCG-AuNPs, or celastrol, at 30% of the respective IC_{50} , for 24, 48, and 72 h, before being stained with acridine orange/ethidium bromide (100 $\mu\text{g}/\text{ml}$; V/V), dissolved in PBS (Baskić et. al 2006). The stained cells were scored under a fluorescence microscope (Axio Imager Z2, Carl Zeiss, Germany) at 200 \times magnification. Cells were classified according to their staining color: live cells were green, apoptotic cells were yellow, and necrotic cells were orange. The experiment was repeated six independent times ($n = 6$), and the mean percentages of live, apoptotic, and necrotic cells were evaluated as the mean \pm SD.

Let-7a and miR34a expression by qRT-PCR

Total RNA was extracted using the miRNeasy RNA extraction kit (217004, Qiagen, Germany) and quantified using a NanoDrop™ 2000 Spectrophotometer (ThermoFisher, MA, USA). Reverse transcription was performed with a miScript RT II RT kit (218161, Qiagen, Germany), using 1 μg of RNA, on a thermocycler (Bioer, PRC), and cDNA was quantified on a NanoDrop™ 2000. PCR amplification was performed using the Stratagene Mx3000p real-time PCR system (Agilent, USA), with the miScript Sybr green PCR kit (218073, Qiagen, Germany). The reaction was performed using 3 ng cDNA and miRNA primers for let-7a (600750, Agilent technologies), miR-34a (MS00003318, Qiagen, Germany), and U6 (600750, Agilent technologies). Relative miRNA expression levels were determined using the $\Delta\Delta\text{Ct}$ method (Livak & Schmittgen 2001), and values were normalized against the expression of U6 in non-treated controls.

Immunocytochemistry of Caspase-3 protein

HepG2 cells were seeded into 8-well cell culture glass slides (SPL life sciences, Korea), at 5×10^3 cells per well. Cells were treated with EGCG-AuNPs (250 and 125 $\mu\text{g}/\text{ml}$) and celastrol (4 $\mu\text{g}/\text{ml}$) for 72 h, prior to fixation with absolute methanol for 20 min. A blocking step was performed using 3% BSA in PBS, for 1 h. Slides were incubated with caspase-3 primary antibody (Ab59388, Abcam), at 4°C overnight, and visualized with Goat anti-Rabbit IgG, Alexa-Fluor-488 (A11034, Invitrogen). Nuclei were counterstained with 1 $\mu\text{g}/\text{ml}$ 4', 6-diamidino-2-phenylindole (DAPI, Sigma). Slides were examined under a fluorescence microscope (Axio Imager Z2, Carl Zeiss, Germany), at 200 \times magnification. The expression of caspase-3 protein was scored and categorized according to the fluorescence intensities (IFU) of the total stained cells per well (grades 1⁺ to 3⁺) relative to non-treated cells (grade 0).

Estimation of the c-Myc anti-apoptotic protein

Cells were treated with EGCG-AuNPs (250 and 125 $\mu\text{g}/\text{ml}$) and celastrol (4 $\mu\text{g}/\text{ml}$) for 72 h. Treated HepG2 cells were lysed (Tansey, 2006), and the total protein content was evaluated using a protein kit (11572, BioSystems). Indirect enzyme-linked immunosorbent assay (ELISA) was used to measure the levels of c-Myc protein in the cell lysate, according to the antibody manufacturer's instructions. c-Myc (C-19) (Sc-788, Santa Cruz Biotechnology) was used as the primary antibody, detected using the Goat Poly Anti-Rabbit IgG (H&L) HRP (K0211708, Koma Biotech) secondary antibody, and EzWay pink-ONE TMB as the substrate solution (K0331070, Koma Biotech). The absorbance was detected with an ELISA-reader, at 450 nm.

Statistical analysis

Experiments were repeated six times, independently ($n=6$), and the data were

expressed as the mean \pm SD. All data were statistically analyzed using a one-way analysis of variance (ANOVA), followed by Dunnett's multiple comparisons test, in Graphpad Prism software, V6. Differences were considered significant when $p < 0.05$.

RESULTS

Characterization of EGCG-AuNPs

The sizes of the prepared EGCG-AuNPs were measured by TEM, which revealed that the prepared nanoparticles were spherical in shape and that the particle size associated with the normal distribution with 35 nm in diameter, on average (Fig. 1b). The absorption spectrum of EGCG-AuNPs was analyzed using ultraviolet (UV)-visible absorption spectroscopy, which showed a maximum absorption (λ_{\max}) of approximately 535 nm, confirming the stability of the molecule (Fig. 1c). The Folin-Ciocalteu colorimetric assay revealed the loading capacity to be $7.8\% \pm 2.3\%$. The relative extinction at 540 nm for EGCG-AuNP revealed no changes in the absorption of EGCG-AuNP in DMEM, either with or without 10% FBS, compared with that of EGCG-AuNP in PBS, after 1 and 24 h.

Antioxidant activity

The antioxidant capacities of EGCG, EGCG-AuNPs, and celastrol for the elimination of DPPH radicals was evaluated in comparison with ascorbic acid (which has high potency for the elimination of free radicals). The antioxidant activity of EGCG-AuNPs, as assessed by the SC_{50} value, was $539 \pm 48 \mu\text{g/ml}$ compared with $45 \pm 1.5 \mu\text{g/ml}$ for EGCG. The SC_{50} value of celastrol was $147 \pm 4 \mu\text{g/ml}$, indicating its low antioxidant activity relative to that of ascorbic acid ($4.7 \pm 0.4 \mu\text{g/ml}$).

Cell viability

HepG2 cells were treated with EGCG and EGCG-AuNPs, at concentrations of 18.75, 37.5, 75, 150, and 300 $\mu\text{g/ml}$, for 24, 48, and 72 h (Fig. 2a and b). EGCG alone, at 300 $\mu\text{g/ml}$, reduced cell viability from 86.87% after 24 h to 68.58% after 72 h. However, when HepG2 cells were treated with EGCG-AuNPs (300 $\mu\text{g/ml}$), cell viability was found to be 72.22%, 69.38%, and 47.64%, after 24, 48, and 72 h, respectively, and the IC_{50} of EGCG-AuNPs was calculated as 254 $\mu\text{g/ml}$ after 72 h. In contrast, HepG2 cells treated with celastrol, as a positive control, at various concentrations (0.625, 1.25, 2.5, 5, and 10 $\mu\text{g/ml}$) for the same time intervals, resulting in significantly increased cytotoxicity at 10 $\mu\text{g/ml}$ at all incubation time points, with cell viability decreasing to 48.64%, 35.15%, and 23.8%, after 24, 48, and 72 h, respectively (Fig. 2c). The IC_{50} value of celastrol was 4 $\mu\text{g/ml}$ after 72 h (Fig. 2).

Apoptosis-Necrosis assay

The cell death pathways involved were investigated by an apoptosis-necrosis assay after culturing HepG2 cells with EGCG, EGCG-AuNP, and celastrol at a concentration equal to 30% of the respective IC_{50} values for 24, 48, and 72 h (Fig. 3). EGCG did not induce apoptotic or necrotic cells in a significant manner compared with non-treated cells, at all investigated time intervals. The percentages of apoptotic cells were elevated gradually when cells were treated with EGCG-AuNPs, reaching $25\% \pm 4.0\%$ after 72 h (Fig. 3b). However, celastrol elevated the percentage of apoptotic cells to $30.67\% \pm 2.0\%$ for the same time interval. Similarly, the necrotic cell percentage increased gradually with increasing exposure duration in cells treated with EGCG-AuNPs and celastrol, reaching $16.00\% \pm 2.7\%$ and $22.33\% \pm 3.0\%$, respectively, compared with non-treated cells ($3.33\% \pm 2.08\%$), at 72 h (Fig. 3b).

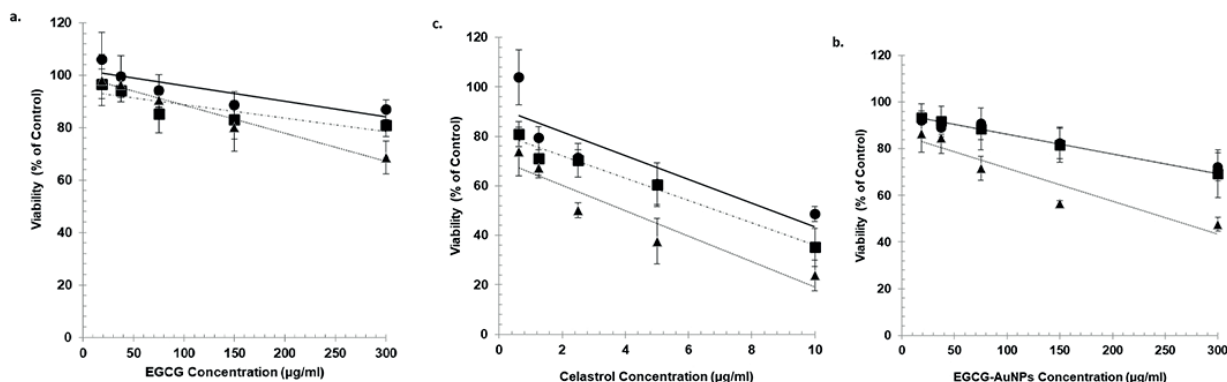


Figure 2. Viability of HepG2 Cells was assessed by MTT assay, after being treated for 24 h (circles), 48 h (squares), and 72 h (triangles) with EGCG (a), EGCG-AuNPs (b) and celastrol (c). Viability is expressed as the percentage of untreated control and presented as the mean ± SD of three independent experiments.

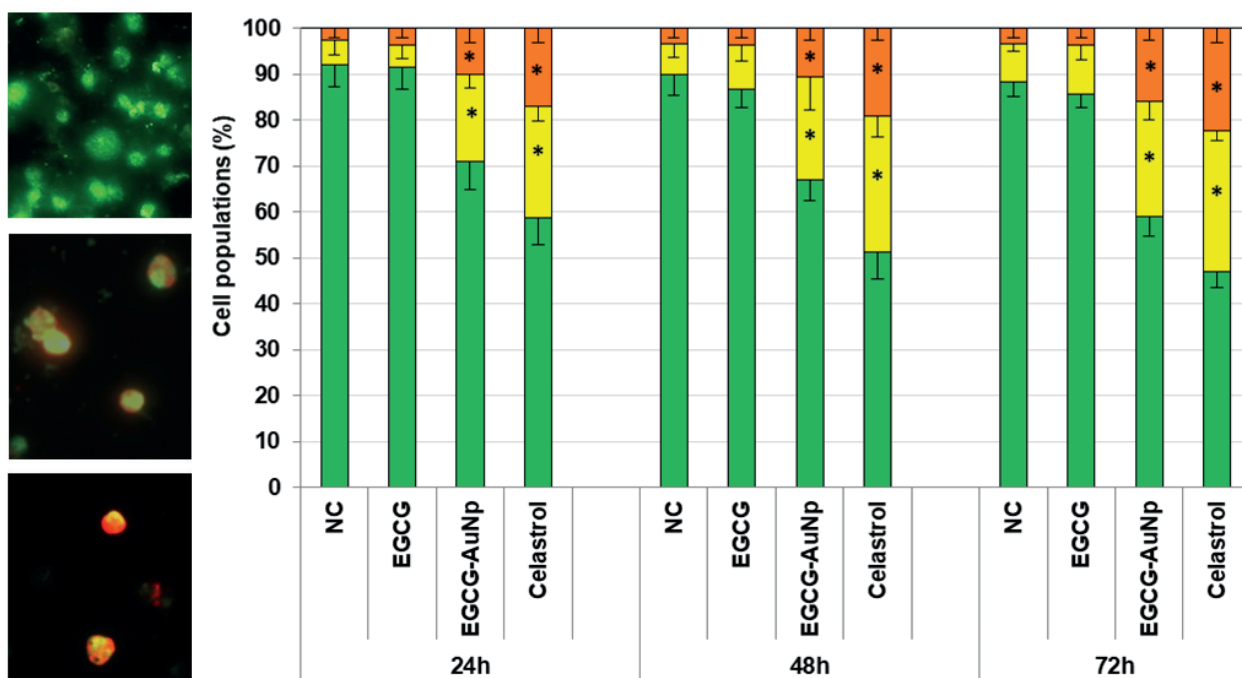


Figure 3. a. Photomicrographs representing control, apoptotic, and necrotic HepG2 cells (from top to bottom). b. A histogram indicates the distribution of vital (green segments), apoptotic (yellow segments), and necrotic (red segments) HepG2 cells, after being treated with 30% of IC_{50} concentrations of EGCG, EGCG-AuNPs, and celastrol, compared with untreated control. Statistical analysis was performed using Graphpad Prism V6.01.*significance compared with untreated control at each respective time point, at $P < 0.05$.

Let7a and miR34a expression

Let-7a and miR-34a are two tumor suppressor miRNAs that are downregulated in tumor cells. Let-7a was significantly elevated in HepG2 cells after treatment with 30% of IC_{50} concentrations of EGCG and EGCG-AuNPs for 72 h, and to 3.67 ± 0.7 ($p < 0.05$) and 7.59 ± 1.7 -fold of the control level ($p < 0.001$), respectively (Fig. 4a). These results indicated a higher potential for EGCG-AuNPs to upregulate Let-7a compared with EGCG alone. Similarly, the treatment with celastrol for 72 h noticeably increased the fold-change in Let-7a expression, up to 9.10 ± 1.4 ($p < 0.001$) (Fig. 4a). In contrast, EGCG and EGCG-AuNPs exhibited similar patterns for the elevation of miR-34a expression, reaching 4.05 ± 0.8 and 3.65 ± 0.6 -fold of the control level (Fig. 4a). Celastrol increased miR-34a expression up to 8.49 ± 1.7 ($p < 0.001$) fold of the control level (Fig. 4a).

c-Myc and Caspase-3

Lysates from cells treated with different concentrations of EGCG-AuNPs and celastrol were used to assess the levels of C-Myc protein, using indirect ELISA. At a low EGCG-AuNP concentration (125 $\mu\text{g}/\text{ml}$), no changes in c-Myc protein levels were observed, whereas, at a high EGCG-AuNP concentration (250 $\mu\text{g}/\text{ml}$) and when treated with celastrol, the c-Myc protein level was significantly reduced ($p < 0.05$) (Fig. 4b). Caspase-3 protein expression levels were elevated when HepG2 cells were treated with EGCG-AuNPs and celastrol, compared with untreated cells after 72 h. In untreated HepG2 cells, the levels of caspase-3 protein expression were low (grade +) (Fig. 5). Caspase-3 protein expression levels elevated gradually with increasing levels of EGCG-AuNPs, reaching grade (++) and grade (+++) at concentrations of 125 $\mu\text{g}/$

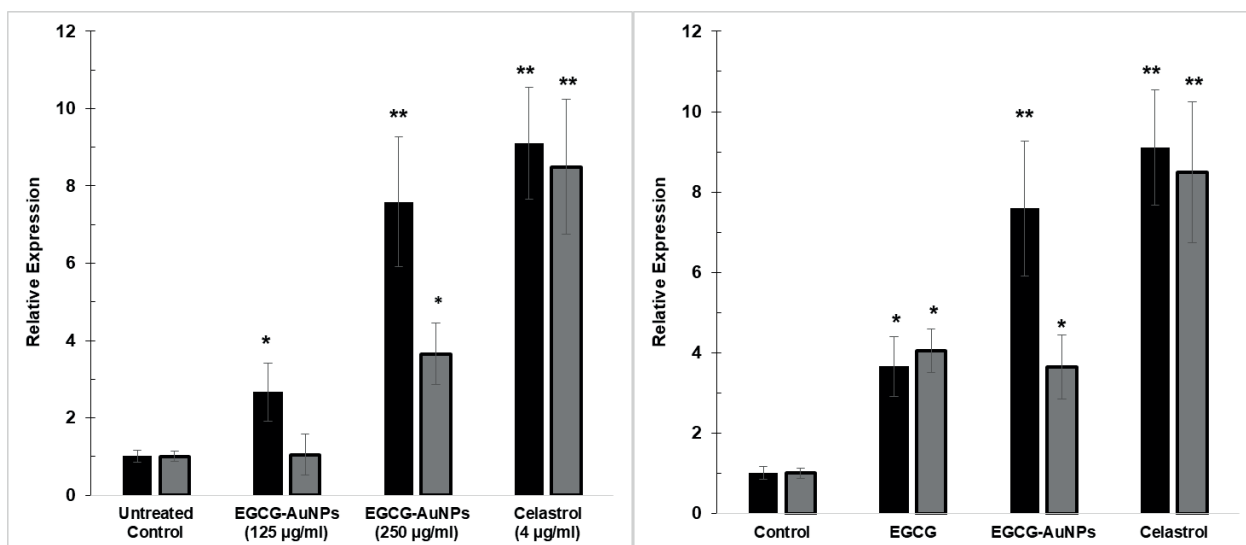


Figure 4. a. Relative expression of let-7a (black bars) and miR-34a (gray bars) in HepG2 cells, after treatment with EGCG-AuNPs and celastrol. **b.** c-Myc protein levels in HepG2 cell lysates, expressed as OD/mg protein/ml, after treatment with EGCG-AuNPs and celastrol, for 72 h, compared with untreated control. Data are presented as the mean \pm SD ($n = 6$). Statistical analysis was performed using Graphpad Prism V6.01. * $p < 0.05$ and ** $P < 0.001$ compared with the corresponding control.

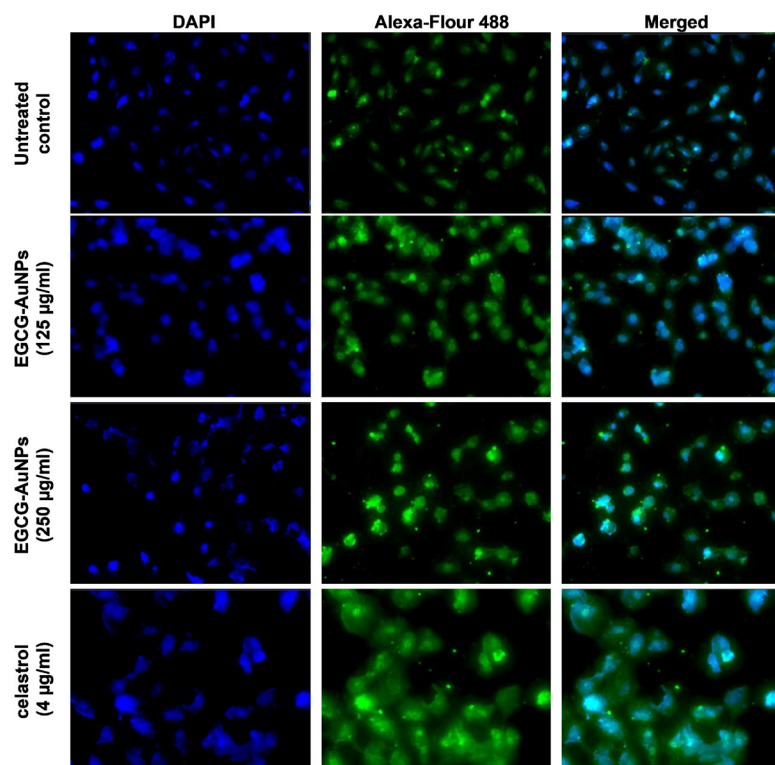


Figure 5. Photomicrographs representing caspase-3 levels in HepG2 cells treated with EGCG-AuNPs and celastrol, compared with the untreated control, after 72 h. HepG2 cells were visualized under fluorescence after being stained with caspase-3-Alexa-Flour-488 (Green) and nuclear counterstaining with DAPI (Blue) (100×).

ml and 250 µg/ml, respectively, whereas grade (+++) was reached when cells were treated with celastrol (Fig. 5).

DISCUSSION

Accumulating evidence shows that EGCG inhibits growth and induces apoptosis in hepatocellular carcinoma cells and liver cancer cells (Du et al. 2012). Our study demonstrated a cytotoxic effect for EGCG alone, in a concentration- and time-dependent manner, with an IC_{50} value of 460 µg/ml after 72 h of treatment, with potent antioxidant activity. In contrast, EGCG-AuNPs showed weak radical-scavenging properties. However, the presence of AuNPs increased the cytotoxic and apoptotic potency of EGCG-AuNPs against HCC. These results agree with the results reported by Hsieh et al. (2019) who found that EGCG conjugated to AuNPs (50-nm diameter) exerted cytotoxic effects on mouse bladder

cancer (MBT-2) cells after 48 h of treatment. The potential and efficacy of EGCG-AuNPs were investigated by Sanna et al. (2011), who reported that loaded EGCG-AuNPs containing small molecules against prostate-specific membrane antigen (PSMA) were able to effectively target prostate cancer cells. Furthermore, Chavva et al. (2019) compared the cytotoxic effects of EGCG-conjugated AuNPs with the effects of citrate-coated AuNPs and EGCG alone on breast cancer MDA-MB-231 cells, prostate cancer PC3 cells, pancreatic MIA PaCa cancer cells, and melanoma A375SM cells, and found that EGCG-conjugated AuNPs possessed superior anticancer activity compared with EGCG alone or with citrate-coated AuNPs, with higher affinity for tumor cells than for normal cells.

In addition to the possible role played by AuNPs, the activity of EGCG-AuNPs may be due to the active structure of EGCG. The chemical formula of EGCG and, in particular, the presence

of the B-ring and D-ring, with multiple hydroxyl groups, could activate the anticancer potency of EGCG-conjugated molecules (Shammas et al. 2006, Li et al. 2011). The structure-function relationship of EGCG demonstrated that the B-ring (Catechol group) possesses potent antioxidant activity, whereas the D-ring (Gallate group) is more effective for inducing cytotoxicity and the inhibition of fatty acid synthase (FASN) in tumor cells, leading to a cytotoxic effect (Braicu et al. 2011; Legeay et al. 2015). This structure-function relationship could explain the EGCG-AuNPs-induced increase in apoptotic cell death and elevated caspase-3 protein expression levels and the downregulation of c-Myc protein, in a concentration-dependent manner, after 72 h. The mechanism of action for EGCG is based on the inhibition of the FASN enzyme (Wang & Tian 2001). FASN is normally present at low levels in normal tissues, where it is responsible for the de novo synthesis of fatty acids, and becomes elevated significantly in HCC (Wang & Tian 2001). EGCG resulted in a dose- and time-dependent decrease in cell viability, which directly correlated with FASN levels, by inducing apoptosis and decreasing the levels of oncoproteins, such as human epidermal growth factor receptor 2 (HER2), protein kinase B (AKT), and extracellular signal-regulated kinase (ERK)1/2 (Puig et al. 2008).

The anticancer properties of EGCG have been confirmed in numerous tumor cell lines and animal models, through the modulation of apoptosis, cell cycle arrest, and angiogenesis, including the regulation of miRNA expression. EGCG is an active regulator of various miRNAs (Shi et al. 2019). In an early study, Tsang et al. (2009) described the influence of EGCG on miRNA expression in human cancer cells. As a result of miRNA microarray analysis, EGCG treatment was found to alter the expression levels of a panel of miRNAs in HepG2 cells. EGCG treatment altered

the expression of at least 61 miRNAs, including the upregulation of miR-1, the Let-7 family, miR-16, miR-18b, miR-20a, miR-25, miR-34a/b, miR-92, miR-93, miR-99a, miR-126, miR-144-3p, miR-182, miR-210, miR-221, miR-320a, miR-330, and miR-498 (Shi et al. 2019, Tsang & Kwok 2009, Kashyap et al. 2019). Our results for EGCG-AuNPs agree with previous reports examining treatment with EGCG treatment alone, and EGCG-AuNPs remarkably upregulated tumor suppressor miRNAs (let-7a and miR-34a), inducing apoptosis through enhanced caspase-3 expression. Let-7 miRNAs are known to act as tumor suppressors and to inhibit HCC cell proliferation and invasion by downregulating MYC and upregulating p16INK (Lan et al. 2011, Wang et al. 2010). These reports demonstrated that the increase in Let-7a expression was consistent with the pro-apoptotic cytotoxic effects caused by the targeting of the c-Myc oncogenic protein by Let-7a. The elevation of miR-34a expression also enhanced apoptosis and cell death (Dang et al. 2013).

Taken together, conjugating EGCG with AuNPs as a nanocarrier accelerates the bioavailability and gradual accumulation of EGCG in cancer cells, inducing cytotoxicity and activating the apoptotic pathway. EGCG-AuNPs upregulated the tumor suppressor miRNAs let-7a and miR34a, which, in turn, upregulated their targeted gene, caspase-3, and downregulated c-Myc protein. This study was the first study to investigate the effects of any AuNPs on miRNA, either capped or uncapped. Further investigations remain necessary to understand the *in vivo* mode of action and delivery of EGCG-AuNPs among biological systems.

Acknowledgments

This work was supported by Taif University Researchers Supporting Project Number (TURSP-2020/103) and the Master Researcher Fund of the National Research Centre, Egypt. We declare no conflicts of interest.

REFERENCES

- AL-SHAELI SJ, ETHAEB AM & BROWN JE. 2019. Anti-neoplastic effect of epigallocatechin gallate on breast cancer cells through glucose metabolism. *J Physics* 1234: 012073.
- BACH DH, HONG JY, PARK HJ & LEE SK. 2017. The role of exosomes and miRNAs in drug resistance of cancer cells. *Int J Cancer* 141: 220-230.
- BADER AG. 2012. miR-34 - a microRNA replacement therapy is headed to the clinic. *Front Genet* 3: 120.
- BASKIĆ D, POPOVIĆ S, RISTIĆ P & ARSENIJEVIĆ NN. 2006. Analysis of cycloheximide-induced apoptosis in human leukocytes: fluorescence microscopy using annexin V/propidium iodide versus acridin orange/ethidium bromide. *Cell Biol Int* 30: 924-932.
- BRAICU C, PILECKI V, BALACESCU O, IRIMIE A & NEAGOE IB. 2011. The Relationships Between Biological Activities and Structure of Flavan-3-Ols. *Int J Mol Sci* 12: 9342-9353.
- CAI H, ZHOU H, MIAO Y, LI N, ZHAO L & JIA L. 2017. MiRNA expression profiles reveal the involvement of miR-26a, miR-548l and miR-34a in hepatocellular carcinoma progression through regulation of ST3GAL5. *Lab Invest* 97: 530-542.
- CHAMUNDEESWARIM, JESLIN J & VERMA ML. 2019. Nanocarriers for drug delivery applications. *Environ Chem Lett* 17: 849-865.
- CHAVVA S, DESHMUKH S, KANCHANAPALLY R, TYAGI N, COYM JW, SINGH AP & SINGH S. 2019. Epigallocatechin Gallate-Gold Nanoparticles Exhibit Superior Antitumor Activity Compared to Conventional Gold Nanoparticles: Potential Synergistic Interactions. *Nanomaterials* 9: pii: E396.
- CHEN J, ZHANG L, LI C, CHEN R, LIU C & CHEN M. 2019. Lipophilized Epigallocatechin Gallate Derivative Exerts Anti-Proliferation Efficacy through Induction of Cell Cycle Arrest and Apoptosis on DU145 Human Prostate Cancer Cells. *Nutrients* 12: 92-96.
- DAIGE CL, WIGGINS JF, PRIDY L, NELLIGAN-DAVIS T, ZHAO J & BROWN D. 2014. Systemic delivery of a miR34a mimic as a potential therapeutic for liver cancer. *Mol Cancer Ther* 13: 2352-2360.
- DANG Y, LUO D, RONG M & CHEN G. 2013. Underexpression of miR-34a in Hepatocellular Carcinoma and Its Contribution towards Enhancement of Proliferating Inhibitory Effects of Agents Targeting c-MET. *PLoS One* 8: e61054.
- DU GJ, ZHANG Z, WEN XD, YU C, CALWAY T, YUAN CS & WANG CZ. 2012. Epigallocatechin Gallate (EGCG) Is the Most Effective Cancer Chemopreventive Polyphenol in Green Tea. *Nutrients* 4: 1679-1691.
- DUBE A, NG K, NICOLAZZO JA & LARSON I. 2010. Effective use of reducing agents and nanoparticle encapsulation in stabilizing catechins in alkaline solution. *Food Chem* 122: 662-667.
- GOLCHIN K, GOLCHIN J, GHADERI S, ALIDADIANI N, ESLAMKHAH S, ESLAMKHAH M, DAVARAN S & AKBARZADEH A. 2018. Gold nanoparticles applications: from artificial enzyme till drug delivery. *Artif Cells Nanomed Biotechnol* 46: 250-254.
- GRANJA A, NEVES AR, SOUSA CT, PINHEIRO M & REIS S. 2019. EGCG intestinal absorption and oral bioavailability enhancement using folic acid-functionalized nanostructured lipid carriers. *Heliyon* 5: e02020.
- GUHRENZ C, WOLF A, ADAM M, SONNTAG L, VOITEKHOVICH SV, KASKEL S, GAPONIK N & EYCHMÜLLER A. 2017. Tetrazole-stabilized gold nanoparticles for catalytic applications. *Z Physik Chem* 231: 51-62.
- HANSEN MB, NIELSEN SE & BERG K. 1989. Re-examination and further development of a precise and rapid dye method for measuring cell growth/cell kill. *J Immunol Methods* 119 :203-10.
- HATA A & LIEBERMAN J. 2015. Dysregulation of microRNA biogenesis and gene silencing in cancer. *Sci Signaling* 8:re3.
- HONG J, LAMBERT JD, LEE SH, SINKO PJ & YANG CS. 2003. Involvement of multidrug resistance-associated proteins in regulating cellular levels of (-)-epigallocatechin-3-gallate and its methyl metabolites. *Biochem Biophys Res Commun* 310: 222-227.
- HSIEH DS, LU HC, CHEN CC, WU CJ & YEH MK. 2012. The preparation and characterization of gold-conjugated polyphenol nanoparticles as a novel delivery system. *Int J Nanomedicine* 7: 1623-1633.
- HSIEH DS, WANG H, TAN SW, HUANG YH, TSAI CY, YEH MK & WU CJ. 2011. The treatment of bladder cancer in a mouse model by epigallocatechin-3-gallate-gold nanoparticles. *Biomaterials* 32: 7633-7640.
- HU J, ZHOU D & CHEN Y. 2009. Preparation and Antioxidant Activity of Green Tea Extract Enriched in Epigallocatechin (EGC) and Epigallocatechin Gallate (EGCG). *J Agric Food Chem* 57(4): 1349-1353.
- KANNAIYAN R, SHANMUGAM MK & SETHI G. 2011. Molecular targets of celastrol derive from Thunder of God Vine: potential role in the treatment of inflammatory disorders and cancer. *Cancer Lett* 303: 9-20.

- KASHYAP N, KUSHWAHA PP, SINGH AK, MAURYA S, SAHOO AK & KUMAR S. 2019. Phytochemicals, Cancer and miRNAs: An in-silico Approach. In: Kumar S., Egbuna C. (eds) *Phytochemistry: An in-silico and in-vitro Update*. Springer, Singapore.
- KHOOBCHANDANI M, KATTI K, MAXWELL A, FAY WP & KATTI KV. 2016. Laminin Receptor-Avid Nanotherapeutic EGCG-AuNPs as a Potential Alternative Therapeutic Approach to Prevent Restenosis. *Int J Mol Sci* 17: 316-320.
- LAMBERT JD & YANG CS. 2003. Cancer chemopreventive activity and bioavailability of tea and tea polyphenols. *Mutat Res Fundam Mol Mech Mutagen* 523-524: 201-208.
- LAN FF, WANG H, CHEN YC, CHAN CY, NG SS, LI K, XIE D, HE ML, LIN MC & KUNG HF. 2011. Hsa-let-7g inhibits proliferation of hepatocellular carcinoma cells by downregulation of c-Myc and upregulation of p16(INK4A). *Int J Cancer* 128: 319-331.
- LEGEAY S, RODIER M, FILLON L, FAURE S, & CLERE N. 2015. Epigallocatechin Gallate: A Review of Its Beneficial Properties to Prevent Metabolic Syndrome. *Nutrients* 7: 5443-5468.
- LI N, TAYLOR LS & MAUER LJ. 2011. Degradation Kinetics of Catechins in Green Tea Powder: Effects of Temperature and Relative Humidity. *J Agri Food Chem* 59: 6082-6090.
- LIVAK KJ & SCHMITTGEN TD. 2001. Analysis of Relative Gene Expression Data Using Real-Time Quantitative PCR and the 2- $\Delta\Delta$ CT Method. *Methods* 25: 402-408.
- LU H, MENG X & YANG CS. 2003. Enzymology of methylation of tea catechins and inhibition of catechol- O -methyltransferase by (-)-epigallocatechin gallate. *Drug Metab Dispos.*; 31:572-579.
- LUO H, TANG L, TANG M, BILLAM M, HUANG T, YU J, WEI Z, LIANG Y, WANG K, ZHANG ZQ, ZHANG L & WANG JS. 2006. Phase IIa chemoprevention trial of green tea polyphenols in high-risk individuals of liver cancer: modulation of urinary excretion of green tea polyphenols and 8-hydroxydeoxyguanosine. *Carcinogenesis* 27: 262-268.
- MERELES D & HUNSTEIN W. 2011. Epigallocatechin-3-gallate (EGCG) for Clinical Trials: More Pitfalls than Promises? *Int J Mol Sci* 12: 5592-5603.
- PANG X, YI Z, ZHANG J, LU B, SUNG B, QU W, AGGARWAL BB & LIU M. 2010. Celastrol suppresses angiogenesis-mediated tumor growth through inhibition of AKT/mammalian target of rapamycin pathway. *Cancer Res* 70: 1951-1959
- PETRICK JL & MCGLYNN KA. 2019. The Changing Epidemiology of Primary Liver Cancer. *Curr Epidemiol Reports* 6: 104-111.
- PUIG T, VÁZQUEZ-MARTÍN A, RELAT J, PÉTRIZ J, MENÉNDEZ JA, PORTA R, CASALS G, MARRERO PF, HARO D, BRUNET J & COLOMER R. 2008. Fatty acid metabolism in breast cancer cells: differential inhibitory effects of epigallocatechin gallate (EGCG) and C75. *Breast Cancer Res Treat* 109: 471-479.
- RAMADASS SK, ANANTHARAMAN NV, SUBRAMANIAN S, SIVASUBRAMANIAN S & MADHAN B. 2015. Paclitaxel/ Epigallocatechin gallate coloaded liposome: A synergistic delivery to control the invasiveness of MDA-MB-231 breast cancer cells. *Colloids Surf B Biointerfaces* 125: 65-72.
- RAMESH N & MANDAL AKA. 2019. Encapsulation of epigallocatechin-3-gallate into albumin nanoparticles improves pharmacokinetic and bioavailability in rat model. *3 Biotech* 9: 238
- SANG S, LAMBERT JD, HO CT & YANG CS. 2011. The chemistry and biotransformation of tea constituents. *Pharmacol Res* 64: 87-99.
- SANNA V, PINTUS G, ROGGIO AM, PUNZONI S, POSADINO AM, ARCA A, MARCEDDU S, BANDIERA P, UZZAU S, SECHI M. 2011. Targeted Biocompatible Nanoparticles for the Delivery of (-)-Epigallocatechin 3-Gallate to Prostate Cancer Cells. *J Med Chem* 54: 1321-1332
- SHAMMAS MA ET AL. 2006. Specific killing of multiple myeloma cells by (-)-epigallocatechin-3- gallate extracted from green tea: Biologic activity and therapeutic implications. *Blood* 108: 2804-2810
- SHI Q, BISHAYEE A & BHATIA D. 2019. Genetic and Epigenetic Targets of Natural Dietary Compounds as Anticancer Agents. *Epigene Cancer Prevent* 8: 3-21.
- SHUKLA R ET AL. 2012. Laminin receptor specific therapeutic gold nanoparticles (198AuNP-EGCG) show efficacy in treating prostate cancer. *Proc Natl Acad Sci USA* 109: 12426-12431.
- SU, YL, LEUNG LK, HUANG Y & CHEN Z-Y. 2003. Stability of tea theaflavins and catechins. *Food Chem* 83: 189-195.
- TANSEY WP. 2006. Freeze-thaw lysis for extraction of proteins from Mammalian cells. *CSH Protoc* 2006: pdb. prot4614.
- TAUBER AL, SCHWEIKER SS & LEVONIS SM. 2020. From tea to treatment; epigallocatechin gallate and its potential involvement in minimizing the metabolic changes in cancer. *Nutr Res* 74: 23-36.
- TSANG WP & KWOK TT. 2009. Epigallocatechin gallate up-regulation of miR-16 and induction of apoptosis in human cancer cells. *J Nutr Biochem* 21: 140-146.
- VAN AMSTERDAM FTM, ROVERI A, MAIORINO M, RATTI E, URSINI F & LACIDIPINE A. 1992. A dihydropyridine calcium antagonist with antioxidant activity. *Free Radic Biol Med* 12: 183-187.

VERMA ML, KUMAR P, SHARMA S, DHIMAN K, SHARMA D & VERMA A. 2020. Gold Nanoparticle-Mediated Delivery of Therapeutic Enzymes for Biomedical Applications. *Nanosci Med* 1: 89-115.

WANG XP, ZHOU J, HAN M, CHEN CB, ZHENG YT, HE XS & YUAN XP. 2017. MicroRNA-34a regulates liver regeneration and the development of liver cancer in rats by targeting Notch signaling pathway. *Oncotarget* 8: 13264-13276.

WANG X & TIAN W. 2001. Green tea epigallocatechin gallate: A natural inhibitor of fatty-acid synthase. *Biochem Biophys Res Commun* 288: 1200-1206.

WANG YC, CHEN YL, YUAN RH, PAN HW, YANG WC, HSU HC & JENG YM. 2010. Lin-28B expression promotes transformation and invasion in human hepatocellular carcinoma. *Carcinogenesis* 31: 1516-1522.

WARDEN BA, SMITH LS, BEECHER GR, BALENTINE DA & CLEVIDENCE BA. 2001. Catechins are bioavailable in men and women drinking black tea throughout the day. *J Nutr* 131: 1731-1737.

YAP J, SLADE D, FOX R, KAUR B, HUGHES A, GANESAN R, VELANGI S & LUESLEY D. 2019. P194 Epivin: a phase II double-blind randomised control trial investigating the use of epigallocatechin-3-gallate (veregen®, catephen®) vs placebo in the treatment of usual-typed vulval intraepithelial neoplasia. *Int J Gynecol Cancer* 29: A173.

YOSHINO K, SUZUKI M, SASAKI K, MIYASE T & SANO M. 1999. Formation of antioxidants from (-)-epigallocatechin gallate in mild alkaline fluids, such as authentic intestinal juice and mouse plasma. *J Nutr Biochem* 10: 223-229.

ZAN L, CHEN Q, ZHANG L & LI X. 2019. Epigallocatechin gallate (EGCG) suppresses growth and tumorigenicity in breast cancer cells by downregulation of miR-25. *Bioengineered* 10: 374-382.

ZAVERI NT. 2006. Green tea and its polyphenolic catechins: Medicinal uses in cancer and noncancer applications. *Life Sci* 78: 2073-2080.

ZHANG B, PAN X, COBB GP & ANDERSON TA. 2007. MicroRNAs as oncogenes and tumor suppressors. *Dev Biol* 302: 1-12.

ZHAO H, XIE P, LI X, ZHU W, SUN X, SUN X, CHEN X, XING L & YU J. 2015. A prospective phase II trial of EGCG in treatment of acute radiation-induced esophagitis for stage III lung cancer. *Radiother Oncol* 114: 351-356.

ZHU QY, ZHANG A, TSANG D, HUANG Y & CHEN ZU. 1997. Stability of green tea catechins. *J Agric Food Chem* 45: 4624-4628.

ZHU S, ZHU L, YU J, WANG Y, WANG Y & PENG B. 2019. Anti-osteoclastogenic effect of epigallocatechin

gallate-functionalized gold nanoparticles in vitro and in vivo. *Int J Nanomedicine* 14: 5017-5032.

How to cite

MOSTAFA SM, GAMAL-ELDEEN AM, EL MAKSOUH NA & FAHMI AA. 2020. Epigallocatechin gallate-capped gold nanoparticles enhanced the tumor suppressors let-7a and miR-34a in hepatocellular carcinoma cells. *An Acad Bras Cienc* 92:e20200574. DOI 10.1590/0001-3765202020200574.

*Manuscript received on April 17, 2020;
accepted for publication on June 17, 2020*

SHADY M. MOSTAFA^{1,2}

<https://orcid.org/0000-0001-8331-6323>

AMIRA M. GAMAL-ELDEEN^{1,2,3}

<https://orcid.org/0000-0002-4423-5616>

NABILA ABD EL MAKSOUH¹

<https://orcid.org/0000-0002-8587-6559>

ABDELGAWAD A. FAHMI⁴

<https://orcid.org/0000-0002-7259-873X>

¹National Research Centre, Biochemistry Department, Genetic Engineering and Biotechnology Division, Dokki, 12622, Cairo, Egypt

²National Research Centre, Cancer Biology and Genetics Laboratory, Centre of Excellence for Advanced Sciences, Dokki, 12622, Cairo, Egypt

³Taif University, Clinical Laboratory Sciences Department, College of Applied Medical Sciences, P.O. Box 11099, 21944, Taif, Saudi Arabia

⁴Cairo University, Chemistry Department, Faculty of Science, Cairo University Rd, 12613, Cairo, Egypt

Correspondence to: **Amira M. Gamal-Eldeen**
E-mail: aeldeen7@yahoo.com, amabdulaziz@tu.edu.sa

Author contributions

Mostafa carried out the biological experiments; Gamal-Eldeen planned and supervised the study, and wrote the manuscript; Abd El Maksoud reviewed the manuscript; and Fahmi carried out the chemical experiments.

